# Nonlinear waves in marginally stable flows of Antarctic Bottom Water

**N I Makarenko[1,2], J L Maltseva[1,2], E G Morozov[3], R Yu Tarakanov[3] and K A Ivanova[4]**

[1] Lavrentyev Institute of Hydrodynamics, Lavrentyev pr. 15, Novosibirsk 630090, Russia
[2] Novosibirsk State University, Pirogova st. 2, Novosibirsk 630090, Russia
[3] Shirshov Institute of Oceanology, Nakhimovski pr. 36, Moscow 117997, Russia
[4] Aix–Marseille University, Marseille 06, France

E-mail: makarenko@hydro.nsc.ru

**Abstract.** In this paper, we study internal waves and stratified flows in the Romanche Fracture Zone of the Mid Atlantic Ridge. Theoretical analysis involves mathematical formulation of stratified flows which uses LADCP- and CTD-data obtained from field observation in the cruises of RV *Akademik Sergey Vavilov*. We discuss the 2.5-layer model of the fluid with exponential stratification of both layers. The long-wave approximate model describing travelling waves is constructed by means of scaling procedure with a small Boussinesq parameter. It is demonstrated that solitary wave regimes can be affected by the Kelvin — Helmholtz instability arising due to interfacial velocity shear in upstream flow.

## 1. Introduction

Deep basins of the Atlantic Ocean are filled with the water of an Antarctic origin which can spread to the mid-latitudes of the Northern Hemisphere [1]. This water is usually called Antarctic Bottom Water (AABW) which means the water mass limited from above by an isotherm of potential temperature 2.0°C. Abyssal water exchange between basins occurs through the fractures of underwater ridges [2]. Our paper is inspired by recent field observations [3] related to extremely long series of internal waves and Kelvin — Helmholtz billows at the equatorial Romanche Fracture Zone of Mid-Atlantic Ridge. This fracture presents an active zone in which a sharp increase in the intensity of the turbulent mixing occurs. Internal waves play significant role here due to the wave breaking which intensifies the mixing. We consider a theoretical model intended to describe internal solitary waves in a two-layer flow with the fluid density depending exponentially on the height in both the layers. The method of derivation involves analysis of the non-linear Dubreil-Jacotin — Long equation that results from stationary Euler equations of stratified fluid. Long-wave scaling procedure uses small Boussinesq parameter which characterizes small slope of the density profile in the layers and small density jump at their interface. This asymptotic procedure combines approaches, applied formerly to pure two-fluid system [4], with perturbation technique developed in the paper [5] for a continuous stratification. Parametric range of solitary wave is considered in the framework of constructed mathematical model. It is demonstrated that these wave regimes can realize to be close to parametric domain of the Kelvin — Helmholtz instability. Such a marginal stability of long internal waves could

explain the formation mechanism of a very long billow trains which intensify the mixing of abyssal waters.

## 2. Basic equations

We consider a 2D motion of inviscid two-layered fluid which is weakly stratified under gravity in each layer. The fully nonlinear Euler equations describing stationary flow are

$$\rho(uu_x + vu_y) + p_x = 0, \quad \rho(uv_x + vv_y) + p_y = -\rho g, \quad u\rho_x + v\rho_y = 0, \quad u_x + v_y = 0, \qquad (1)$$

where $\rho$ is the fluid density, $(u, v)$ is the fluid velocity, $p$ is the pressure and $g$ is the gravity acceleration. It is supposed that the flow is confined between the flat bottom $y = -h_1$ and the rigid lid $y = h_2$ (see Figure 1). The layers are separated by the interface $y = \eta(x)$ having the equilibrium level $y = 0$.

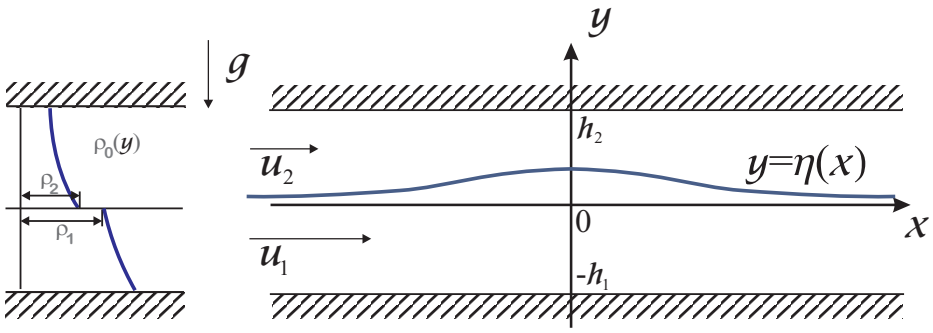


**Figure 1.** Scheme of the flow

Looking for a solitary-wave solutions, we require the fluid velocity $(u, v)$ to attain the upstream velocity $(u_j, 0)$ as $x \to -\infty$. Non-disturbed parallel flow has no vertical velocity and elevation (i.e. $v = 0$, $\eta = 0$) but the horizontal velocity $u = u_0(y)$ may be piece-wise constant, so we have $u_0(y) = u_1$ by $-h_1 < y < 0$, and $u_0(y) = u_2$ by $0 < y < h_2$. Upstream fluid density $\rho = \rho_0(y)$ and the pressure $p = p_0(y)$ should be coupled by the hydrostatic equation $dp_0/dy = g\rho_0$. We consider the density profile depending exponentially on height,

$$\rho_0(y) = \begin{cases} \rho_1 \exp\left(-N_1^2 y/g\right) & (-h_1 < y < 0), \\ \rho_2 \exp\left(-N_2^2 y/g\right) & (0 < y < h_2), \end{cases} \qquad (2)$$

where $N_j = \text{const}$ is the Brunt — Väisälä frequency in $j$-th layer, and the constants $\rho_1$ and $\rho_2$ are such that $\rho_2 < \rho_1$.

It is known [6] that stationary system (1) can be reduced to single scalar equation for a stream function $\psi$ defined by formulae $u = \psi_y$, $v = -\psi_x$. Namely, the fluid density $\rho$ can be determined from the upstream condition by the relation $\rho(\psi) = \rho_0(\psi/u_j)$ in the $j$-th layer. By that, excluding the pressure $p$ from (1) leads to the non-linear Dubreil-Jacotin — Long (DJL) equation

$$\Delta\psi = \frac{N_j^2}{gu_j}\left\{g\left(y - \frac{\psi}{u_j}\right) + \frac{1}{2}\left(|\nabla\psi|^2 - u_j^2\right)\right\}, \qquad (3)$$

where $\Delta = \partial_x^2 + \partial_y^2$ is the Laplace's operator, $\nabla = (\partial_x, \partial_y)$; the indexes $j$ should be taken $j = 1$ in lower layer, and $j = 2$ in upper layer. Kinematic boundary conditions at the bottom, at interface and at the lid have the form, respectively

$$\psi = -u_1 h_1 \ \ (y = -h_1), \qquad \psi = 0 \ \ (y = \eta), \qquad \psi = u_2 h_2 \ \ (y = h_2). \qquad (4)$$

In addition, the continuity of the pressure $p$ provides the nonlinear boundary condition at unknown interface

$$2g(\rho_1-\rho_2)\eta=\rho_2(|\nabla\psi|^2-u_2^2)|_{y=\eta(x)+0}-\rho_1(|\nabla\psi|^2-u_1^2)|_{y=\eta(x)-0}. \tag{5}$$

## 3. Non-linear long-wave model

We introduce non-dimensional independent variables $\bar{x}$, $\bar{y}$ and functions $\bar{\eta}$, $\bar{\psi}$ by the formulae

$$(x,y,\eta)=\frac{h_1}{\pi}\,(\bar{x},\bar{y},\bar{\eta}),\quad \psi=\frac{u_jh_j}{\pi}\,\bar{\psi}$$

considered separately in the lower layer ($j=1$) or in the upper layer ($j=2$). Using the ratio of undisturbed thicknesses of the layers $r=h_1/h_2$, we locate the bottom as $\bar{y}=-\pi$, and relation $\bar{y}=\pi/r$ defines the rigid lid. Scaling procedure involves dimensionless parameters

$$F_j=\frac{u_j}{\sqrt{g_jh_j}},\quad \sigma_j=\frac{N_j^2h_j}{\pi g},\quad \lambda_j=\frac{N_jh_j}{\pi u_j}\quad (j=1,2);\quad \mu=\frac{\rho_1-\rho_2}{\rho_2}.$$

Here, the densimetric (or internal) Froude number $F_j$ presents scaled fluid velocity $u_j$ in the $j$-th layer, defined with reduced gravity acceleration $g_j=(\rho_1-\rho_2)g/\rho_j$. The Boussinesq parameters $\sigma_1$, $\sigma_2$ characterize the slope of the density profile (3) in continuously stratified layers, and the Atwood number $\mu$ determines the density jump at interface. The Long's numbers $\lambda_j$ are not independent, these constants are coupled with the parameters $\sigma_1$, $\sigma_2$, $\mu$ and $F_j$ by the relations

$$\lambda_1^2=\frac{\pi\sigma_1(1+\mu)}{\mu F_1^2},\quad \lambda_2^2=\frac{\pi\sigma_2}{\mu F_2^2}. \tag{6}$$

Parameters $\sigma_1$, $\sigma_2$ and $\mu$ are small in the case of low stratification. However, the limit passage $\sigma_j\to 0$, $\mu\to 0$ is singular because the Long's numbers $\lambda_j$ involve the ratios $\sigma_j/\mu$ in formulae (6). The 2.5-layer model uses the hypotheses that the Boussinesq parameters $\sigma_1$, $\sigma_2$ and the Atwood number $\mu$ are of the same order, so we can use a single small parameter $\sigma$ by setting

$$\sigma=\sigma_1=\sigma_2=\mu. \tag{7}$$

In accordance with hypothesis (7), the derivation procedure of long-wave model should involve the slow horizontal variable $\xi=\sqrt{\sigma}\,\bar{x}$, as it was demonstrated originally by Benney & Ko (1978) in the case of slight linear stratification. Thus, we obtain the equations for scaled stream function $\bar{\psi}$ and non-dimensional wave elevation $\bar{\eta}$ as follows (bar is omitted throughout what follows):

$$\sigma\psi_{\xi\xi}+\psi_{yy}+\lambda_1^2\,(\psi-y)=\frac{1}{2}\,\sigma\left(\sigma\psi_\xi^2+\psi_y^2-1\right)\qquad(-\pi<y<\eta(\xi)) \tag{8}$$

$$\sigma\psi_{\xi\xi}+\psi_{yy}+\lambda_2^2r^2\,(\psi-ry)=\frac{1}{2}\,\sigma\left(\sigma\psi_\xi^2+\psi_y^2-r^2\right)\qquad(\eta(\xi)<y<\pi/r) \tag{9}$$

Kinematic boundary conditions (4) can be rewritten now as follows:

$$\psi(\xi,-\pi)=-\pi,\quad \psi(\xi,\eta(\xi))=0,\quad \psi(\xi,\pi/r)=\pi. \tag{10}$$

Correspondingly, Eq. (5) providing continuity of pressure at interface $y=\eta(x)$ takes the form

$$2\eta=F_2^2(\sigma\psi_\xi^2+\psi_y^2-r^2)|_{y=\eta+0}-F_1^2(\sigma\psi_\xi^2+\psi_y^2-1)|_{y=\eta-0}. \tag{11}$$

We find the stream function $\psi$ to be expanded in a power series with respect to $\sigma$ as

$$\psi = \psi^{(0)}(\xi, y) + \sigma\,\psi^{(1)}(\xi, y) + ... \tag{12}$$

where the leading-order term $\psi^{(0)}$ defines the hydrostatic mode, and the coefficient $\psi^{(1)}$ provides the correction due to non-linear dispersion. These coefficients are uniquely determined via the wave elevation $\eta$ by the equations (8)–(10), so we obtain

$$\psi^{(0)}(\xi, y) = \begin{cases} y - \eta\,\dfrac{\sin\lambda_1(\pi + y)}{\sin\lambda_1(\pi + \eta))} & (-\pi < y < \eta), \\ ry - r\eta\,\dfrac{\sin\lambda_2(\pi - ry)}{\sin\lambda_2(\pi - r\eta)} & (\eta < y < \pi/r), \end{cases}$$

where $\lambda_j = 1/\sqrt{\pi}F_j$ $(j = 1, 2)$ should be taken at the leading order in $\sigma$ in accordance with formulae (6) and (7). The dispersive term $\psi^{(1)}$ is much more complicated, but it can be calculated also in explicit form via the function $\eta$. Now we substitute power expansion (12) for function $\psi$ into the condition (11) and truncate the terms with the powers higher than the first power of $\sigma$. By that, we obtain the first-order ordinary differential equation for the wave elevation $\eta(x)$ as

$$\left(\frac{d\eta}{dx}\right)^2 = \eta^2\,\frac{D(\eta; F_1, F_2)}{Q(\eta; F_1, F_2)} \tag{13}$$

where function $D$ is given by the formula

$$D(\eta; F_1, F_2) = \sqrt{\pi}F_1\,\mathrm{ctg}\left\{\frac{\pi + \eta}{\sqrt{\pi}F_1}\right\} + \sqrt{\pi}F_2\,\mathrm{ctg}\left\{\frac{\pi - r\eta}{\sqrt{\pi}F_2}\right\} + \frac{1}{3}\,(1 - r)\eta - 1.$$

Denominator $Q$ in (13) has one more complicated form, so we refer to the paper [7] for details. The model equation (13) generalizes the non-linear models early suggested in [4,8,9] for a system with constant densities in both layers, as well as the latest "2.5-layer" models considered in [10-12].

Solitary-wave solutions of Eq. (13) are given in the implicit form by the formula

$$x = \pm \int_a^\eta \sqrt{\frac{Q(s; F_1, F_2)}{D(s; F_1, F_2)}}\,\frac{ds}{s} \tag{14}$$

where parameter $a$ determines non-dimensional amplitude of the wave. Parametric range of solitary waves described by Eq. (13) is formed by the domain in $(F_1, F_2)$-plane where the radical function $Q/D$ in (14) is ensured to be non-negative. The function $Q(s; F_1, F_2)$ is positive in the vicinity of point $s = 0$; therefore, function $D$ plays the determining role here. Depending on $F_1$ and $F_2$, this function can change the sign even by small $s$. As a consequence, the map of solitary-wave regimes is formed by the Froude numbers $(F_1, F_2)$ such that inequality $D(0; F_1, F_2) > 0$ holds. This inequality defines the range of non-linear waves, which are supercritical with respect to the phase speed of linear harmonic wave-packets. Spectrum of normal modes, defined on the $(F_1, F_2)$-plane, is demonstrated on Figure 2 (left panel), where modal bounds are formed by separate branches of the curve

$$\sqrt{\pi}\,F_1\,\mathrm{ctg}\frac{\sqrt{\pi}}{F_1} + \sqrt{\pi}\,F_2\,\mathrm{ctg}\frac{\sqrt{\pi}}{F_2} = 1.$$

The domain covered only by the first mode is marked here with the blue color. Correspondingly, the embedded domain of the second mode is highlighted with the yellow, and the third mode is marked with the pink color. The range of internal solitary waves is shown in the right panel of Figure 2, this is the narrow band marked by the orange color. The narrowness of this range reveals anomalously low amplitude dispersion of solitary waves described in the framework of considered 2.5-layer model of a weakly stratified fluid.

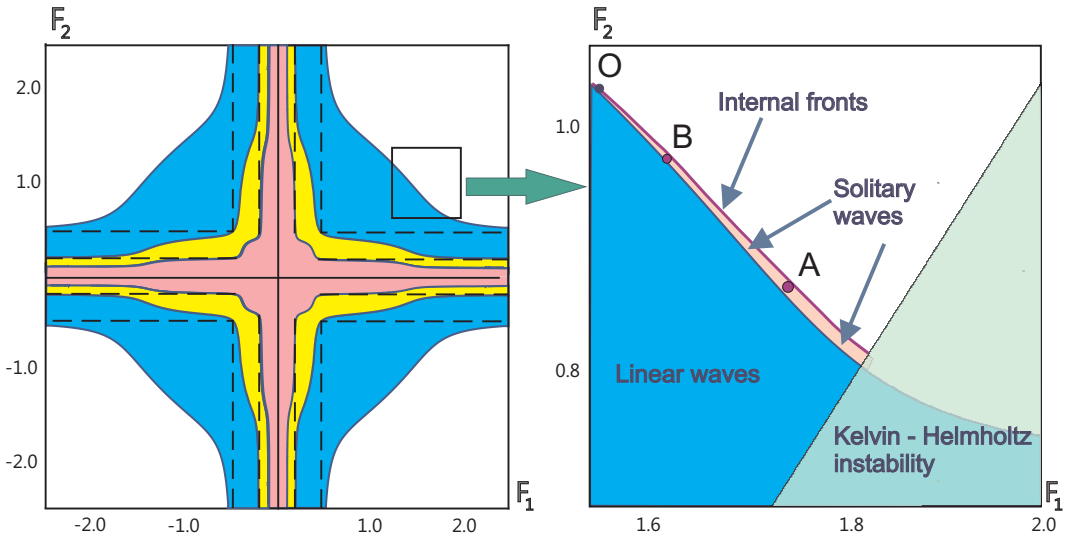


**Figure 2.** Spectrum of linear waves (colored modes 1-3) (left) and fragment of parametric domain of solitary waves (right).

## 4. Flows of Antarctic Bottom Water in the Romanche Fracture Zone

We present in this Section a comparison of solutions of Eq. (13) with the field data measured for internal solitary waves in weakly stratified abyssal currents. Figure 3 demonstrates fragments of temperature distribution in a quasi-steady shear bottom flow recorded from mooring station with a 350-m line of thermistors located over a depth of 4720 m at the entrance to the Romanche Fracture Zone in the equatorial Atlantic [3]. Trains of short-period (20÷30 min) internal waves modulated by tide propagate here along a sharp interface corresponding to the 0.85°C isotherm which separates the lower layer of cold Antarctic Bottom Water (AABW) from the overlying warmer AABW layer with temperature $\theta < 2.0$°C. Moored temperature and velocity data show permanently marginal stability of the flow with the Richardson numbers $0.25 < \mathrm{Ri} < 1$. In this context, internal Froude numbers $F_1$ and $F_2$ characterize the magnitude of the velocity jump at the interface in upstream flow. The shear $u_1 \neq u_2$ between the layers initiate the development of the Kelvin — Helmholtz instability which provides non-stationary formation of billow trains [13] Long-wave perturbations give the greatest contribution to this instability due to their increased power intensity. Constant two-layer flow is linearly stable in the long-wave limit if the inequality

$$|u_1 - u_2| < \sqrt{\frac{g(\rho_1 - \rho_2)(\rho_1 h_2 + \rho_2 h_1)}{\rho_1 \rho_2}} \tag{15}$$

holds, and this flow is unstable in the opposite case. Exactly the same bound (15) follows from the *non-linear* stability criteria predicted by the shallow water theory ([14]; see also [15]) for a *variable* difference $|u_1 - u_2|$ and *variable* layer thicknesses $h_1$ and $h_2$. Tidal amplification of the shear triggers the formation of small-scale overturns which create long trains of the Kelvin — Helmholtz billows.

Bold curves in Figure 3 show overlapped profiles of internal waves calculated from (14). The upstream parameters used in the calculation were chosen from CTD and LADCP data of density and currents measured immediately at the fronts of solitary waves. Upstream velocities $u_1$, $u_2$ were assumed as $u_1 = 35 \div 45\ cm/s$ and $u_2 = 10 \div 20\ cm/s$. These values correspond to the mean velocities measured in the western part of the Romanche Fracture Zone by a velocity LADCP

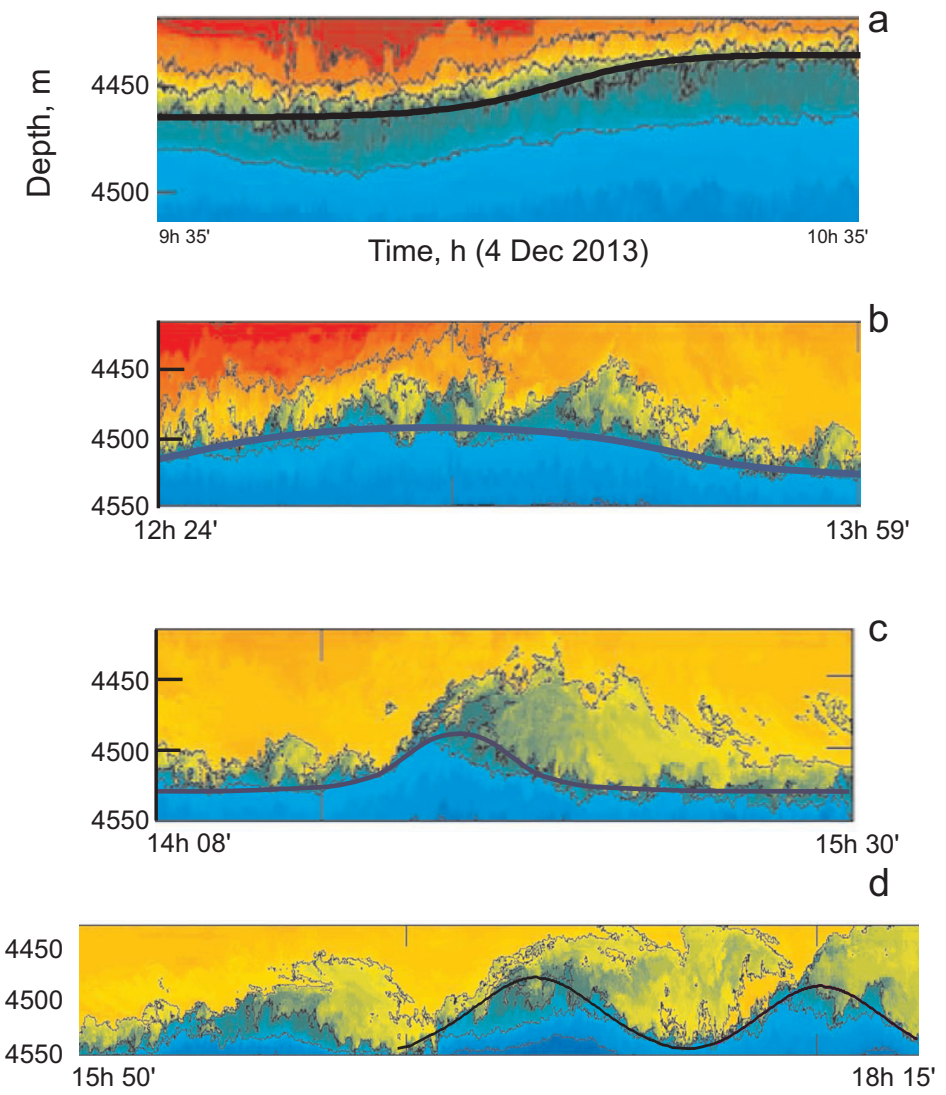


**Figure 3.** Internal waves in AABW flows affected by the Kelvin — Helmholtz instability

profiler in the cruises of the R/V "Akademik Sergey Vavilov" [16] and measured on the mooring station [3]. Maximal velocity of the flow in the lower layer, recorded by the mooring station within 6 months is as high as 65 $cm/s$. That intense shear is induced here by the permanent inflow of bottom waters to the fracture zone through a narrow gap in its southern wall.

Figure 3a demonstrates front-like wave (smooth internal bore) affected by moderate small-scale shear instability. The non-dimensional amplitude of this wave is $a = \eta_{max}/h_1 = 0.16$, and calculated solution corresponds to the Froude point A with coordinates $(F_1, F_2) = (1.719, 0.891)$ shown in Figure 2 (right panel). Point A belongs to the bore diagram which is tangential to the spectrum boundary at the point O. Figure 3b demonstrate a long series of overturns which are distributed uniformly along with gently sloped wave top. It is interesting that similar overturning near the middle part of broad solitary wave was observed in laboratory experiments [17]. In contrast, solitary wave shown on Figure 3c is relatively short, and the flow is apparently non-symmetric due to intensive breaking which localizes downstream the sharp wave-crest. Figure 3d demonstrates the train of three subsequent solitary waves with intense overturns in the lee side

of these waves. The amplitude of the leading wave shown in Figure 3d is clearly lower than the amplitudes of the following two waves, which occur randomly and are almost identical. The solitary-wave type of these two waves corresponds to Froude point B with coordinates $(F_1, F_2) = (1.634, 0.959)$.

## 5. Acknowledgments

This work was supported by the grants of the Russian Foundation for Basic Research (project nos. 17-08-00085, 18-01-00648) and Interdisciplinary Program II.1 of SB RAS (project No 2). Roman Tarakanov was supported by the Russian Science Foundation (grant No 16-17-10149).

## 6. References

[1] Mantyla A W and Reid J L 1983 Abyssal characteristics of the World Ocean waters *Deep-Sea Res.* **30** 805-833
[2] Morozov E, Demidov A, Tarakanov R and Zenk W 2010 *Abyssal Channels in the Atlantic Ocean: Water Structure and Flows* (Dordrecht: Springer)
[3] Van Haren H, Gostiaux L, Morozov E and Tarakanov R 2014 Extremely long Kelvin — Helmholtz billow trains in the Romanche Fracture Zone *Geophys. Res. Lett.* **44**(23) 8445–8451
[4] Ovsyannikov L V, Makarenko N I, Nalimov V I et al 1985 Nonlinear Problems of the Theory of Surface and Internal Waves, (Novosibirsk: Nauka) [in Russian]
[5] Benney D J and Ko D R S 1978 The propagation of long large amplitude internal waves *Stud. Appl. Math.* **59** 187-199
[6] Yih C-S 1980 *Stratified Flows* (New York: Academic Press)
[7] Makarenko N, Maltseva J, Tarakanov R and Ivanova K 2018 Internal solitary waves in a layered weakly stratified flow *The Ocean in Motion* (Dordrecht: Springer) 55–66
[8] Miyata M 1985 An internal solitary wave of large amplitude *La Mer* **23** 43–48
[9] Choi W and Camassa R 1999 Fully nonlinear internal waves in a two-fluid system *J.Fluid Mech.* **396** 1–36
[10] Voronovich A G 2003 Strong solitary internal waves in a 2.5- layer model *J. Fluid Mech.* **474** 85–94
[11] Makarenko N I and Maltseva J L 2009 Phase velocity spectrum of internal waves in a weakly-stratified two-layer fluid *Fluid Dyn.* **44**(2) 278–294
[12] Makarenko N I and Maltseva J L 2009 Solitary waves in a weakly stratified two-layer fluid *J. Appl. Mech. Techn. Phys.* **50**(2) 229–234
[13] Thorpe S A 1985 Laboratory observations of secondary structures in Kelvin — Helmholtz billows and consequences for ocean mixing *Geophys. Astrophys. Fluid Dyn.* **34** 175–190
[14] Ovsyannikov L V 1979 Two-layer shallow water model *J. Appl. Mech. Tech. Phys.* **20** 127–135
[15] Gavrilyuk S L, Makarenko N I and Sukhinin S V 2017 *Waves in continuous media* (Cham, Switzerland: Birkhäuser/ Springer)
[16] Tarakanov R Yu, Makarenko N I and Morozov E G 2013 Antarctic bottom water flow in the western part of the Romanche Fracture Zone based on the measurements in October of 2011 *Oceanology* **53**(6) 655–667
[17] Grue J, Jensen A, Rusås P-O and Sveen J K 2000 Breaking and broadening of internal solitary waves *J.Fluid Mech.* **413** 181–217